
Proceedings Paper:
Smith, A.F., Thanarak, J., Pontin, M. et al. (2 more authors) (2021) Design and development of a robotic bioreactor for in vitro tissue engineering. In: Proceedings of 2021 IEEE International Conference on Robotics and Automation (ICRA 2021). IEEE International Conference on Robotics and Automation (ICRA 2021), 30 May - 05 Jun 2021, Xi'an, China. IEEE (Institute of Electrical and Electronics Engineers) , pp. 12428-12434.

https://doi.org/10.1109/ICRA48506.2021.9560728

Design and Development of a Robotic Bioreactor for In Vitro Tissue Engineering

Abigail F. Smith[1], Jeerawan Thanarak[2], Marco Pontin[1], Nicola H. Green[2 3], and Dana D. Damian[1]

***Abstract*— In this study, a novel robotic bioreactor is presented with capabilities of closed-loop control of force and displacement applied to a tissue scaffold and tissue scaffold stiffness calculation. These characteristics bring the potential of a robotic bioreactor that can optimize the mechanical properties of tissue constructs in order for them to match those of native tissues. Custom position and force control signals are designed to maintain a steady tensioning of the tissue scaffold while the latter one's mechanical properties evolve in time. We propose a simple model to support the hypothesis that the stiffness of a cell-seeded scaffold increases over time, and thus force control signals need to be adjusted accordingly. The robotic bioreactor is able to measure the stiffness of a scaffold sample relatively accurately, with an average standard deviation of 0.2N/mm. The combination of accurate stiffness measurements and a closed-loop control system equips the robotic bioreactor with the fundamental requirements to achieve stiffness based force control in future in vitro experiments, and thus to a tissue-scaffold responsive technology for advanced tissue engineering.**

I. INTRODUCTION

In vitro testing offers a platform to perform more detailed analysis of cells or tissues that would not be possible with a whole organism, whilst also having the ethical advantage of avoiding animal testing. It can help explain, with greater detail, isolated behaviour of tissue or cells and form a clearer picture into how that behaviour contributes to the organism. *In vitro* testing can also determine testing conditions for later *in vivo* experiments, such as with implantable devices.

Cells respond to mechanical stimuli [1]. The stimuli can induce proliferation, differentiation, apoptosis, or secretion of extracellular matrix (ECM) deposition [2]. This mechanostimulation can be taken advantage of to develop therapies, such as novel robotic implants that apply tension to esophageal tissue to encourage cell growth and reconstruct missing tissue areas of the organ [3]. Research into optimum mechanostimulation regimes are vast and suggest that different regimes induce different results. The types of cell and environment used can also affect the results of a study, including cell proliferation capability and ECM production [4][5]. All these variables, however, require long and time consuming iterative experiments in search of globally optimum conditions, as current tissue engineering tools are limited by a lack of sensing and adaptive control methods.

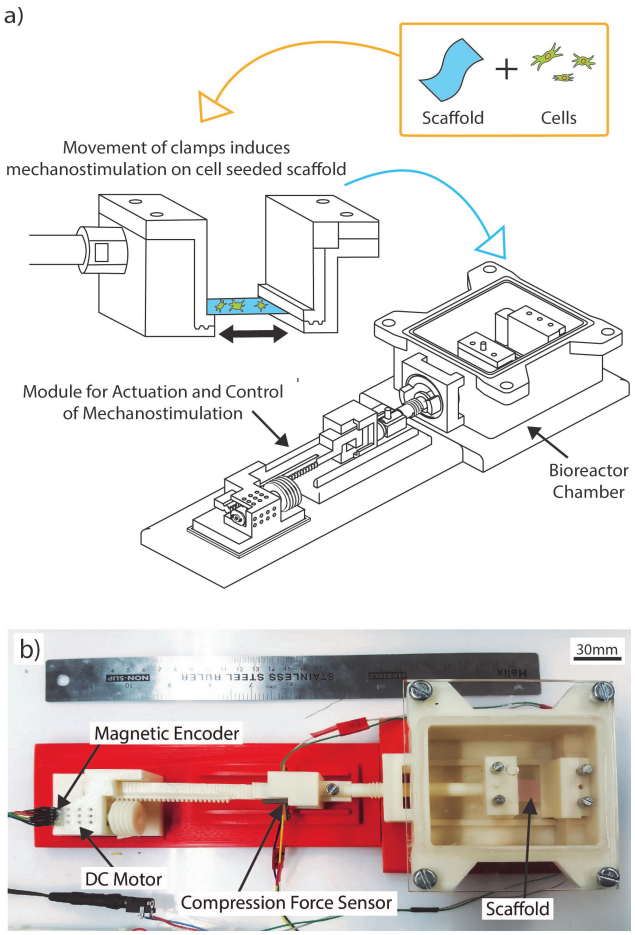

Fig. 1. Robotic bioreactor. a) Illustration of the protocol that will be followed to validate the bioreactor in an *in vitro* experiment. b) Image of the robotic bioreactor.

II. RELATED WORK

While tissue engineering has great potential in constructing tissues and organs from scratch, there are multiple challenges recognised in the field, including identifying the optimum protocol to stimulate a population of cells so they develop in a way that recreates the geometrical and mechanical properties of the target native tissue [6]. Bioreactors are used in tissue engineering to mimic and regulate the environment of the cells during *in vitro* experimentation. Cells are seeded for mechanical support in a biomaterial and are bathed in a nutrient medium. Mechanical stimulation is

[1] Department of Automatic Control and Systems Engineering, University of Sheffield, S1 3JD, United Kingdom, e-mails: afsmith1@sheffield.ac.uk, d.damian@sheffield.ac.uk

[2] Department of Material Science and Engineering, University of Sheffield, S1 3JD, United Kingdom

[3] INSIGNEO Institute for In Silico Medicine, The Pam Liversidge Building, Sir Robert Hadfield Building, Mappin Street, Sheffield, UK

This work was partially funded by The United Kingdom Engineering and Physical Sciences Research Council (EPSRC) ERC DTP Scholarship and The Royal Thai Government.

applied either through tensioning, pressure or fluidic shear. Commerical bioreactors that induce mechanical stimulation, such as Ebers TC-3 Bioreactor [7], BioTense [8], Cartigen [9], are regularly used in tissue engineering. Results from experiments using commercial bioreactors have shown increases in extracellular matrix (ECM) deposition and cell proliferation [4][10][11]. The ECM is a non-cellular complex network that provides structural support to the cells and determines the stiffness of the tissue [12].

Other research groups have also developed their own bioreactor to suit the needs of their experiments. In particular, in [13], a bioreactor utilizes force sensors in its design to monitor the force throughout experiments. They do not, however, use this force data to alter the stimulation applied to the cell-seeded scaffold (CSS) during the experiment. With most bioreactors, including the ones previously mentioned, once the program has been set, there is no change to the programme during the experiment. This means there is no recognition that the global mechanical properties of the system changes over time, leading to the research question: if the global system is changing its own mechanical properties, should the mechanical stimulation applied to the scaffold also adapt?

The robotic bioreactor design proposed in this paper, focuses on the application of tissue-engineering fundamentals into an autonomous robot to encourage the creation of a different tissue which resembles native tissue on a CSS. The motivation for this study comes from the hypothesis that if a CSS is changing its mechanical properties throughout the experiment, then a force required to deliver a true constant mechanical stimulation also changes.

The aim of this paper is to present the theoretical and practical benchtop validation of a 3D printed robotic bioreactor. The study will introduce the fundamental requirements to enable stiffness-based force control in *in vitro* experiments in order to achieve optimisation of the mechanical properties of tissue constructs. The contributions of this paper are (1) the design and development of a novel robotic bioreactor with scaffold tension and displacement sensing; (2) the development towards custom stiffness-adaptive force and position control; (3) the proposal of a future protocol needed to validate the bioreactor *in vitro*.

III. MECHANICAL DESIGN

The robotic bioreactor consists of mainly two parts: (1) a sterilizable assembly where the cells are kept in biological conditions, and (2) a non-sterilizable assembly dedicated to the sensing of the CSS and control of the robotic bioreactor. This design allows the merging of a typical protocol of *in vitro* cell seeding and a post-seeding control setup.

A. Sterilizable Assembly

1) Chamber: The foundation of any bioreactor is that the cells should be able to survive and thrive within the chamber and so a sterile environment must be maintained. The chamber is fabricated with Acrylonitrile butadiene styrene (ABS) using a fused deposition modeling (FDM) 3D printing technique. The chamber measures 116mm $\times$ 55mm $\times$ 88mm, with a lid sealing the chamber measuring 120mm $\times$ 105mm laser cut from 6mm thick acrylic sheet. Furthermore, during *in vitro* experiments clean sterile air needs to be pumped inside the chamber and constantly recycled during the experiment. A $0.22\ \mu m$ filter is used to facilitate gas transfer between incubator and the cell culture environment. To accommodate this filter, a hole was laser cut in the lid (Fig.3a). The filter would be added under the class 2 biological cabinet after the chamber and its counterparts have been sterilized.

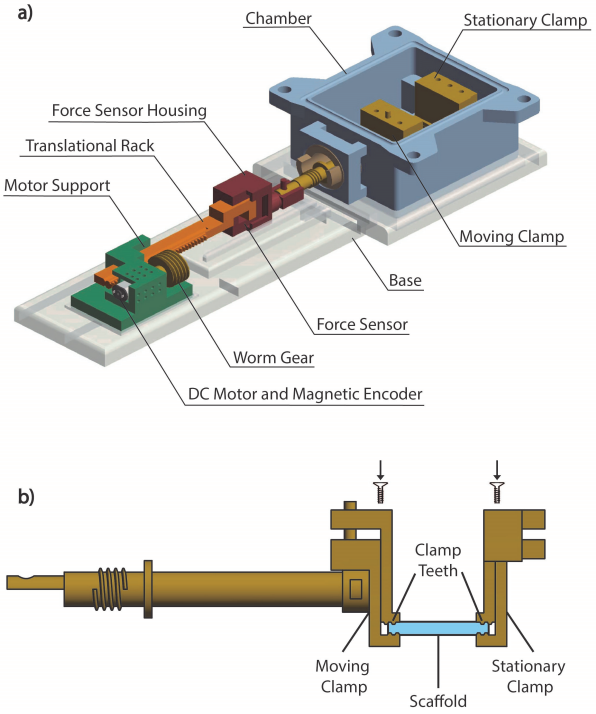

Fig. 2. CAD design of the robotic bioreactor. a) Main components of the robotic bioreactor; b) Details of the robotic bioreactor clamps. The clamp teeth grip the scaffold and hold it in place whilst mechanical stimulation is applied. They are engaged by tightening the bolts at the top of the clamp.

Cell medium is added into the chamber to encourage and maintain cell survival, growth and replication whilst preventing contamination. In order to make the chamber water impermeable, the inside of the chamber is melted with acetone. A custom sealing ring is fabricated from Ecoflex 00-30 and placed on the top margins of the chamber to ensure that the lid is sealed and air tight. Four nuts and bolts are used to secure the lid at the four corners of the chamber.

2) Clamps: The CSS is held by two ABS clamps produced by rapid prototyping and feature teething patterns for a secure grip of the scaffold as shown in Fig.2b. While one clamp is fixed to the wall of the chamber with screws (distal clamp), the other one is driven by the external control module along a linear direction to pull and relax the scaffold (proximal clamp). The clamps, not including the rod which is attached to the clamp (proximal), measures 35mm $\times$ 38mm

$\times$ 18mm. The moving clamp (proximal) is supported by the chamber floor which as designed with built-in tracks. These tracks inhibit the lateral movement of the clamp, which is likely to damage and tear the scaffold, while minimising the friction between the two elements. The clamp teeth are designed to grip the scaffold evenly to distribute the force across the scaffold as localised force is likely to damage the scaffold. The process of clamping the CSS is performed under a class 2 biological cabinet. This has contributed significantly to the design of the clamps so that the clamping can be performed using only sterilized tools to reduce the risk of contamination to the chamber and CCS.

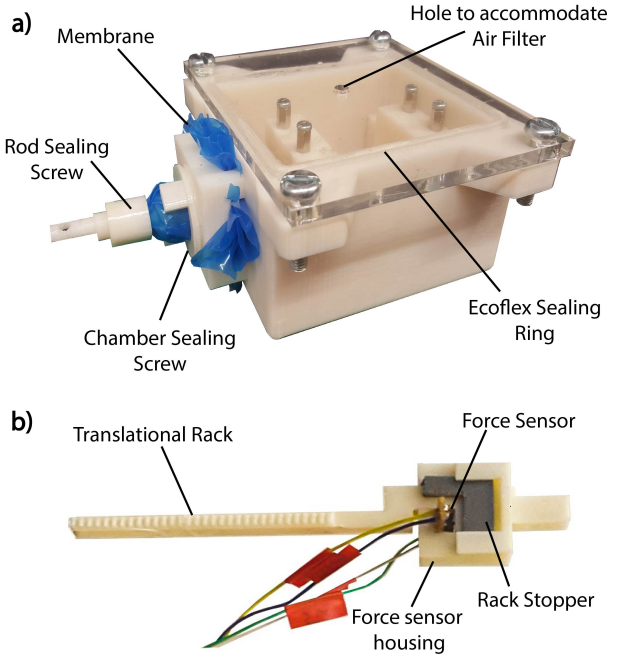

Fig. 3. Details of the robotic bioreactor a) The chamber. A membrane keeps the chamber water tight and prevents contaminants to enter the sterile chamber, which is kept in place by the rob sealing screw and chamber sealing screw. The hole in the lid is to accommodate for the air filter during *in vitro* experiments. b) Force sensor mounting mechanics. The force sensor is soldered onto a breadboard and then glued to the force sensor housing so that the 'hook' of the rack engages with the force sensor when the scaffold is tensioned. The rack stopper is used to stop the hook misaligning with the force sensor.

3) Sealing membrane: The clamp (proximal) exits the chamber through a hole in the chamber wall, which creates an entrance for contaminants to enter from the external environment into the chamber. It is crucial to isolate the chamber from the external environment. This has been done by using a separating polyurethane membrane of 0.4mm thickness (Fig. 3a). The membrane is attached to the outside of the chamber using a thread and a counterpart to the thread that tightly screws around the membrane to maintain a strong grip against the junction. The second part of the membrane is attached to the rod using the same threading and screw mechanism. The membrane has been tested successfully against leakage by filling the chamber with medium (pink color), leaving it for 3 days and visually surveying for any leaks.

B. Non-sterilizable Assembly

The actuation module is placed outside of the sterile chamber and encompasses electronic components that would not withstand the sterilization process required for the chamber. The actuation module enables the linear displacement of the proximal clamp in the chamber. A DC-motor-driven worm gear, with a pitch of 1.95mm, meshes to a teethed rod which is connected to the proximal clamp. This module is placed outside of the chamber.

A mechanism was designed to accommodate a compression force sensor that can detect the amount of force applied to the scaffold through each pulling cycle. This sensor was soldered to a protoboard and then was placed and glued between the hook of the teethed rack and the rod of the proximal clamp (Fig.3b).

The base of the robotic bioreactor features tracks to avoid lateral deflections during the linear motion of the rod. The bioreactor and base fit into an area measuring 343mm $\times$ 110mm $\times$ 63mm, so will fit in most conventional incubators that provide the required environmental conditions for cell survival.

IV. Electrical Design

The mechanical stimulation of the scaffold is driven by a 12V DC microgear motor (Pololu) with a magnetic encoder placed at the back of the rotor. The motor has a 297.92:1 gear ratio which actuates the worm-gear mechanism. This actuation chain implies an important ratio r between one motor rotation (sensed by the encoder) and an actual rack translation. We can calculate that one step of the encoder senses a 0.00056mm moving of the clamps. From calibration we measure a 0.0006mm movement of the rack from one step in the encoder. The relative error of this ratio is $e = \frac{|r_{exp} - r_{th}|}{r_{th}} = 9\%$.

A force sensor (Honeywell FSS005WNGT) is used in combination with an amplifier (INA121P), which has a sensing range of 0N to 5N. The force sensor was sampled every 25ms. The force sensor was calibrated with calibrated weights. The controller is implemented on an Arduino MEGA powered from a laptop. Since the sensor is the connection point between the upstream section of the actuation chain (i.e. the motor) and the rod of the clamp that is pulling the scaffold, the force sensed is approximately equal to the actual force applied onto the scaffold. Friction forces do exist between the moving elements of the bioreactor and only contribute to a minor difference between the actual force applied to the scaffolds and the sensed force.

V. Control

A. Cell-Seeded Scaffold Evolution

The CSS and its material properties evolve in time and the resulting material properties are the consequence of a combination of scaffold degradation, cell proliferation and ECM deposition [2][14][15]. If a scaffold is biodegradable, its mass will reduce along with its material properties over time [16]. At the same time, ECM is being deposited by

the cells which contributes to new material properties of the system, such as tensile strength and stiffness [14]. In this study, we consider scaffold degradation and collagen production to mainly contribute to the stiffness of the global system. For future *in vitro* study, Poly(glycerol sebacate)-Methacrylate (PGSM) will be used as the scaffold. PGSM is a photocurable Poly(glycerol sebacate) (PGS) produced by functionalization with methacrylate groups [16]. PGSM exhibits linear degradation over time at a rate of 20% mass loss at 30 days [16][17]. We assume that a loss of mass of the scaffold will affect material properties, such as a reduction in tensile strength and stiffness. It is therefore predicted that the stiffness is likely to reduce 4.7% over a week long experiment. In [2], experimental results show that cells seeded on PGSM scaffold secreted 50% more collagen than cells growing in 6 well tissue culture plastic plates (control) over a 7 day *in vitro* experiment. ECM determines the stiffness of tissue [12]. Given that we predict a relatively small change in the stiffness of PGSM, we hypothesise that it will have a small impact on the overall stiffness of the CSS at the end of a 7-day experiment. As collagen is found in the ECM, the increase in collagen also indicates an increase in overall ECM deposition and will result in an overall increase of stiffness of the tissue scaffold. To stimulate the cells in a three-dimensional environment, the force needs to be large enough for the cells to sense and react to it [18] and if the global stiffness increases, as we predict it to, the cells will require a greater force to sense the same mechanostimulation signal throughout the experiment.

B. Scaffold mechanostimulation control

1) Position and force control: While typical bioreactors have predefined open loop control, due to changes that occur in the CSS, it is imperative to have a cue of the evolution of the scaffold and be able to adjust the control signals accordingly. For the position control, a sinusoidal target waveform is set with a frequency of 0.25Hz, an amplitude of 3mm and an offset of 3mm to achieve maximum displacement of 6mm and minimum displacement of 0mm. The initial position of the clamps were remotely changed with buttons to control the motor to ensure that the scaffold was pre-tensioned the same amount in each trial.

For force control, a sinusoidal target waveform is set, with a frequency of 0.25Hz, an increasing amplitude starting at 0.4N and an offset that also increases at the same rate at the amplitude to keep the reference signal above 0N. Frequencies of 0.1Hz to 1Hz have been used to stimulate fibroblasts in previous studies, so we chose 0.25Hz for our reference signal to sit within this range [19][20][5]. Both the position control and force control was implemented in Arduino using a PD controller and tuned accordingly. The force sensor readings were filtered with a moving average filter in post processing. A phantom scaffold, fabricated from Ecoflex 00-30, measuring 30mm $\times$ 10mm $\times$ 4mm was used in both the position and force control experiments.

2) Stiffness calculation: Previously, it was discussed that the stiffness of the global system is likely to increase over time. If the stiffness of the CSS is computed at regular intervals throughout a 7-day experiment, we can track how the CSS is changing over time. This parameter can also be used to control the force applied to the scaffold. As the CSS stiffens, a greater force is needed to maintain a constant mechanostimulation. The stiffness of the cell-seeded scaffold can be calculated as:

$$S_s = \frac{F_s}{E_s} \tag{1}$$

where S_s is the stiffness of scaffold, F_s is the force on scaffold and E_s is the elongation of scaffold, as transduced by the sensors in the system.

The stress-strain relationship of the phantom scaffolds was obtained with a uniaxial tensile test on an electric static testing instrument (MX2, IMADA). Two samples of Ecoflex (Ecoflex 00-10 and Ecoflex 00-30) were prepared, measuring 30mm $\times$ 10mm $\times$ 4mm and one sample of PGSM, measuring 10mm $\times$ 25mm $\times$ 1mm. Both Ecoflex samples were pulled at a constant speed of 1 mm/sec and the PGSM sample was pulled at a rate of 0.7mm/sec. The Ecoflex samples were pulled to 15mm displacement to ensure we test within the elastic region of the Ecoflex. The PGSM was pulled to 3.5mm displacement, beyond which its breaking point is reached. Each of the Ecoflex samples was tested three times, first with the bioreactor and then with the IMADA. One trial was conducted with PGSM sample. Force measurements for both the IMADA and bioreactor were filtered using a moving average in post processing.

VI. Experiments and Results

We tested the capability of the robotic bioreactor to control the displacement and force applied to tissue scaffolds, as well as validate the stiffness calculation. These tests were conducted without cells and using materials such as elastomers as proxy for the scaffold, as well as a biomaterial that is eligible for in vitro tissue engineering.

A. Position and Force control

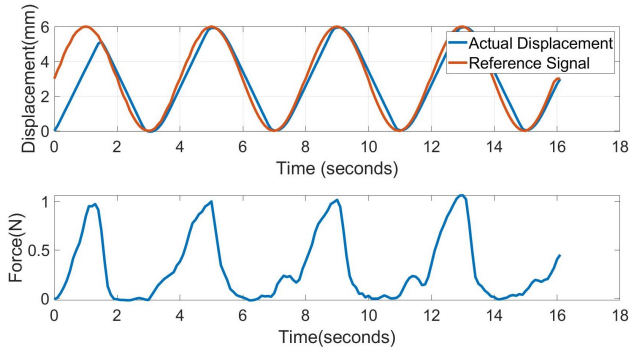

Fig. 4. Displacement control of the scaffold. (Top) The position control signal (red) shows the desired trajectory of the clamp displacement compared to the actual displacement of the clamps (blue). (Bottom) Force sensor readings during position control experiment.

In Fig. 4, the desired trajectory of the position control is shown as a sinusoidal waveform. Following the peaks in the

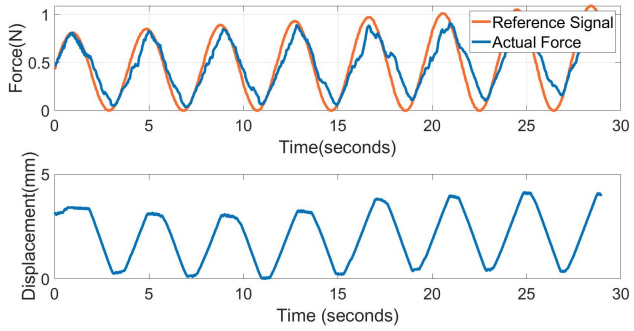

Fig. 5. Force control of the scaffold. (Top) The force control signal (red) shows the desired trajectory of the force measured by the force sensor compared to the actual force readings (blue). (Bottom) Displacement of the clamps from their original position during force control experiment.

force sensor reading, a sharp drop in force is shown. This is expected as the force sensor is only being compressed when the clamp is pulling the scaffold in tension. When the clamp direction is reversed, there are no compression forces acting on the force sensor. The secondary peaks that occur at approximately 7 and 11 seconds are likely a result of the combination of the viscoelastic behaviour of the phantom scaffold and sensitivity of the force sensor.

In Fig. 5, we show a desired force trajectory compared to the actual force measured by the force sensor. We see a general trend of the force sensor reading following the trajectory and the position of the rack in response to the force control. The amplitude of the target force signal increases over time which is achieved by increasing the displacement of the scaffold until the desired force is achieved. The behaviour demonstrates the potential behaviour of stiffness-based force control; when the stiffness of the CSS increases over time, the force applied to the scaffold also increases so that a constant force is applied to the scaffold throughout the experiment.

B. Stiffness Calculation

1) Stiffness calculation validation with tensile test machine: Fig. 6 shows that the bioreactor measurements follow the trend of the tensile testing machine with the average standard deviation of the mean for the bioreactor measurement calculated as 0.10N/mm for Ecoflex 00-10 and 0.37N/mm for Ecoflex 00-30.

Fig. 7 shows the clamps following a ramp trajectory, until the scaffold has been displaced 3.5mm. At 14% stretch, the PGSM reaches its tensile limit. This is shown by the sharp increase in force at 3.3mm displacement.

2) Stiffness derivation during mechanostimulation regimen: In this experiment, the stiffness calculation process for long-term *in vitro* experimentation using position control is demonstrated. We see in Fig. 8 how the displacement follows a sinusoidal function and then after two cycles, the displacement follows a ramp function. This ramp function is necessary to statically calculate the stiffness of the scaffold in real time. If the stiffness was calculated during normal mechanostimulation, we are likely to include damping and elastic behaviour in the measurements without accounting for it mathematically.

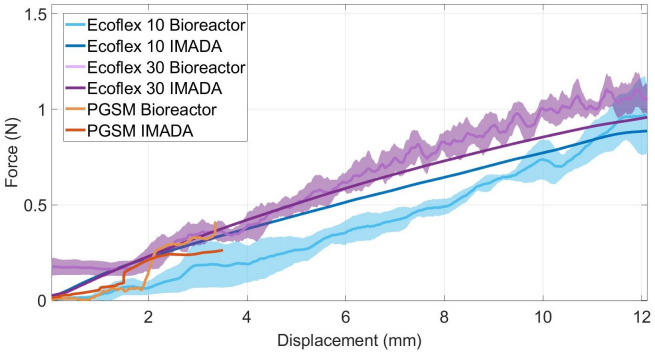

Fig. 6. Tensile testing of the robotic bioreactor compared to the IMADA tensile testing machine. The mean (bold line) and standard deviation (shaded area) of the three trials are plotted for Ecoflex 00-10 and 00-50. The bold line with no shaded region are the mean of three trials for each of the Ecoflex samples tested with the IMADA tensile testing machine. The red and orange line are results for the PGSM scaffold tensile test conducted by the IMADA tensile testing machine and the robotic bioreactor respectively.

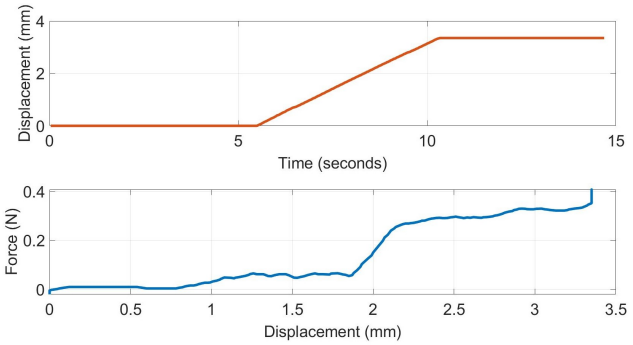

Fig. 7. Example of a control signal for stiffness calculation. (Top) Displacement of the PGSM scaffold following a ramp signal controlled by the position controller. The controller displaces the pre-tensioned scaffold to 3.5mm at a steady rate of 0.7mm/sec and then stops. (Bottom) Force and displacement measurements from the bioreactor during the ramp displacement.

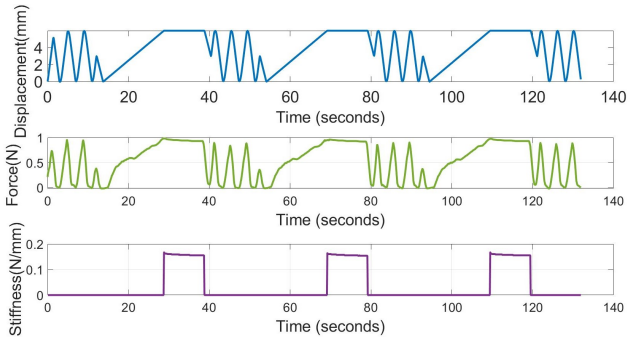

Fig. 8. Example of the robotic bioreactor's capabilities to enable mechanical stimulation of the tissue scaffold and derive its stiffness during its operation. (Top) The displacement of the rack following a sinusoidal waveform (blue) interspersed with ramp function at regular intervals. (Middle) Force measurements taken throughout experiment. (Bottom) A stiffness measurement is calculated at the same timestamp as when the ramp reaches its maximum displacement for 10 seconds.

VII. In Vitro Protocol

The following protocol was designed for future experimentation to validate the bioreactor (Fig.9). PGSM scaffolds will be seeded with human dermal fibroblasts under aseptic conditions and cultured in a humidified incubator at 37°C, 5% CO2 to adhere to the scaffold for 24 hours. Once seeded, the scaffolds will be divided into three sets; one two-dimensional (2D) control, one 3D scaffold with no mechanical stimulation applied and one 3D scaffold with mechanical stimulation applied by the robotic bioreactor. To provide the cells with nutrition, 25 ml of medium will then added into the chamber. The medium will be prepared by combining Dulbecco's modified eagle's medium (DMEM) with Fetal Calf Serum, penisilin, fungizone and glutamine. The first set will be stimulated by the robotic bioreactor, the second set will be stimulated by Ebers [7] (as reference) and the last two scaffolds will be used as a 3D control. The 2D control will be proceeded by seeding the same number of cells onto tissue culture plastic (TCP) and will be placed in the same incubator. This 2D control will be used as the reference as the cells can be visually observed using a microscope.

For the case of the bioreactor introduced in this paper, the scaffolds used need to provide sufficient structural support for the cells [21], whilst maintaining elastic properties and resilience against wear [22][23] or plastic behaviour [24].

Sterility of the bioreactor is ensured through disinfecting all components and tools after every experiment. The ABS material of the chamber cannot be autoclaved since autoclave temperatures are higher than the ABS melting point[25]. Consequently, to disinfect the bioreactor, 70% isopropanol will be used since it is reported to disinfect more thoroughly in comparison with 70% ethanol [26].

The experiment will run over multiple days in the controlled environment; at body temperature (37°C), 5% CO_2, 21% O_2 and 0% humitidy (to protect the electrical components within the bioreactor). Two different assays will be used to evaluate the performance of stimulation; resazurin, to acquire the metabolic rate of the cells [27], and picrosirius red assay, to determine collagen production [28].

Preliminary testing of the robotic bioreactor was conducted with a CSS mounted to the clamps and then placed inside an incubator along with four CSS in a petridish, one CSS in the Ebers bioreactor [7] (Fig.9). From this 3 days static experiment, it was verified that the chamber of the bioreactor was able to maintain a sterile environment from visual inspection of the cell media in comparison to the other controls. The viability of using the electronic components within an incubator was confirmed from this experiment as the components were still functional after 3 days.

VIII. Discussion and Conclusions

In this paper, we introduce the concept of a novel robotic bioreactor equipped with the fundamental requirements to achieve stiffness-based force control in the future and validate these features with benchtop experiments. It is crucial to have a validation before moving forward with *in vitro* experiments, as there are more variables that can affect the results in such experiments.

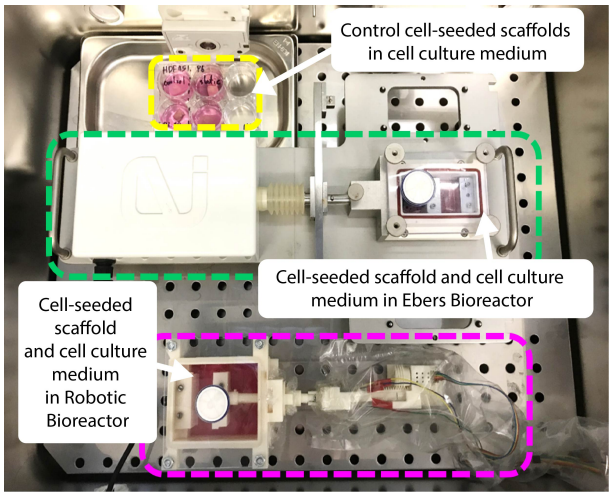

Fig. 9. Experimental set up to validate the chambers ability to maintain a sterile environment within an incubator for 3 days. Control CCS in petri dish (yellow), CCS in Ebers [7] (green) and CCS in the Robotic Bioreactor (pink).

The robotic bioreactor is able to administer a variety of stimulation regimes, including those not achieved by commercially available bioreactors, such as an intermittent and incremental sinusoidal waveforms.

This 3D printed bioreactor can be adapted to be used for compression stimulation as opposed to tension stimulation, as demonstrated in this paper, with design changes to the chamber and clamps only. Limitations of 3D printing centre around poor dimensional accuracy when printing parts such as the worm gear. Future iterations of the bioreactor will include using a combination of 3D printed parts for elements of the bioreactor that is advantageous to change between experiments, such as the chamber and clamps and non-3D printed parts where accuracy is crucial, such as the worm gear and rack.

Implementing two different controllers into the bioreactor demonstrates its versatility as a tool. The position control appeared to be more robust than the force control as was less noise in the encoder readings than there was for the force sensor. The force control, however, is a novel approach to induce mechanostimulation onto a CSS. Both control methods can be used to achieve stiffness-based control which may be a step closer to achieving optimum mechanostimulation for CCS where the force applied to the an evolving scaffold is truly constant throughout an experiment.

The next steps include the validation of the mechanostimulation signals of the robotic bioreactor to regulate and optimise the cell-seeded scaffold *in vitro* in week-long experiments.

Acknowledgment

We thank Theo LeSignor, Hiba Khalidi for early prototypes of this technology, and Baoqiang Jia for his input to the work.

REFERENCES

[1] A. W. Orr, B. P. Helmke, B. R. Blackman, and M. A. Schwartz, "Mechanisms of mechanotransduction," *Developmental Cell*, vol. 10, no. 1, pp. 11 – 20, 2006.

[2] J. Thanarak, H. Mohammed, S. Pashneh-Tala, F. Claeyssens, and N. Green, "Enhanced collagen production from human dermal fibroblasts on poly (glycerol sebacate)-methacrylate scaffolds," in *2018 11th Biomedical Engineering International Conference (BMEiCON)*. IEEE, 2018, pp. 1–4.

[3] D. D. Damian, K. Price, S. Arabagi, I. Berra, Z. Machaidze, S. Manjila, S. Shimada, A. Fabozzo, G. Arnal, D. Van Story *et al.*, "In vivo tissue regeneration with robotic implants," *Science Robotics*, vol. 3, no. 14, p. eaaq0018, 2018.

[4] B. Lohberger, H. Kaltenegger, N. Stuendl, B. Rinner, A. Leithner, and P. Sadoghi, "Impact of cyclic mechanical stimulation on the expression of extracellular matrix proteins in human primary rotator cuff fibroblasts," *Knee Surgery, Sports Traumatology, Arthroscopy*, vol. 24, no. 12, pp. 3884–3891, 2016.

[5] J. B. Schmidt, K. Chen, and R. T. Tranquillo, "Effects of Intermittent and Incremental Cyclic Stretch on ERK Signaling and Collagen Production in Engineered Tissue," *Cellular and Molecular Bioengineering*, vol. 9, no. 1, pp. 55–64, 2016.

[6] A. Atala, F. K. Kasper, and A. G. Mikos, "Engineering complex tissues," *Science Translational Medicine*, vol. 4, no. 160, pp. 160rv12–160rv12, 2012.

[7] Tc-3 bioreactor. [Online]. Available: https://ebersmedical.com/tissue-engineering/bioreactors/load-culture/tc-3

[8] Biotense bioreactor. [Online]. Available: https://www.admet.com/products/micro-testers/biotense-bioreactor/

[9] Cartigen: Mechanical compression bioreactor systems. [Online]. Available: http://www.tissuegrowth.com/prod_cartilage.cfm

[10] S. Yano, M. Komine, M. Fujimoto, H. Okochi, and K. Tamaki, "Mechanical stretching in vitro regulates signal transduction pathways and cellular proliferation in human epidermal keratinocytes," *Journal of Investigative Dermatology*, vol. 122, no. 3, pp. 783–790, 2004.

[11] H. Iwasaki, S. Eguchi, H. Ueno, F. Marumo, and Y. Hirata, "Mechanical stretch stimulates growth of vascular smooth muscle cells via epidermal growth factor receptor," *American Journal of Physiology-Heart and Circulatory Physiology*, vol. 278, no. 2, pp. H521–H529, 2000.

[12] L. D. Muiznieks and F. W. Keeley, "Molecular assembly and mechanical properties of the extracellular matrix: A fibrous protein perspective," *Biochimica et Biophysica Acta (BBA) - Molecular Basis of Disease*, vol. 1832, no. 7, pp. 866 – 875, 2013, fibrosis: Translation of basic research to human disease.

[13] C. A. Cook, P. Y. Huri, B. P. Ginn, J. Gilbert-Honick, S. M. Somers, J. P. Temple, H. Q. Mao, and W. L. Grayson, "Characterization of a novel bioreactor system for 3D cellular mechanobiology studies," *Biotechnology and Bioengineering*, vol. 113, no. 8, pp. 1825–1837, 2016.

[14] J. K. Lee, L. W. Huwe, N. Paschos, A. Aryaei, C. A. Gegg, J. C. Hu, and K. A. Athanasiou, "Tension stimulation drives tissue formation in scaffold-free systems," *Nature Materials*, vol. 16, no. 8, pp. 864–873, 2017.

[15] B. S. Kim, J. Nikolovski, J. Bonadio, and D. J. Mooney, "Cyclic mechanical strain regulates the development of engineered smooth muscle tissue," *Nature Biotechnology*, vol. 17, no. 10, pp. 979–983, 1999.

[16] S. Pashneh-Tala, R. Owen, H. Bahmaee, S. Rekštyte, M. Malinauskas, and F. Claeyssens, "Synthesis, characterization and 3D micro-structuring via 2-photon polymerization of poly(glycerol sebacate)-methacrylate-an elastomeric degradable polymer," *Frontiers in Physics*, vol. 6, no. MAY, 2018.

[17] I. Pomerantseva, N. Krebs, A. Hart, C. M. Neville, A. Y. Huang, and C. A. Sundback, "Degradation behavior of poly(glycerol sebacate)," *Journal of Biomedical Materials Research Part A*, vol. 91A, no. 4, pp. 1038–1047, 2009.

[18] Y. Cui, F. M. Hameed, B. Yang, K. Lee, C. Q. Pan, S. Park, and M. Sheetz, "Cyclic stretching of soft substrates induces spreading and growth," *Nature Communications*, vol. 6, no. 1, p. 6333, 2015.

[19] R. Kuang, Z. Wang, Q. Xu, S. Liu, and W. Zhang, "Influence of mechanical stimulation on human dermal fibroblasts derived from different body sites," Department of Plastic and Aesthetic Surgery, The Affiliated Hospital of Qingdao University Qingdao 266003, Shandong, China., pp. 7641–7647, 2015.

[20] S. D. Waldman, C. G. Spiteri, M. D. Grynpas, R. M. Pilliar, and R. A. Kandel, "Long-term intermittent shear deformation improves the quality of cartilaginous tissue formed in vitro," *Journal of Orthopaedic Research*, vol. 21, no. 4, pp. 590 – 596, 2003.

[21] G. Vunjak-Novakovic, B. Obradovic, I. Martin, P. M. Bursac, R. Langer, and L. E. Freed, "Dynamic cell seeding of polymer scaffolds for cartilage tissue engineering," *Biotechnology progress*, vol. 14, no. 2, pp. 193–202, 1998.

[22] S.-H. Lee, B.-S. Kim, S. H. Kim, S. W. Choi, S. I. Jeong, I. K. Kwon, S. W. Kang, J. Nikolovski, D. J. Mooney, Y.-K. Han *et al.*, "Elastic biodegradable poly (glycolide-co-caprolactone) scaffold for tissue engineering," *Journal of Biomedical Materials Research Part A: An Official Journal of The Society for Biomaterials, The Japanese Society for Biomaterials, and The Australian Society for Biomaterials and the Korean Society for Biomaterials*, vol. 66, no. 1, pp. 29–37, 2003.

[23] Y. Lei and Z. Ferdous, "Design considerations and challenges for mechanical stretch bioreactors in tissue engineering," *Biotechnology progress*, vol. 32, no. 3, pp. 543–553, 2016.

[24] B. Gong, S. Cui, Y. Zhao, Y. Sun, and Q. Ding, "Strain-controlled fatigue behaviors of porous pla-based scaffolds by 3d-printing technology," *Journal of Biomaterials Science, Polymer Edition*, vol. 28, no. 18, pp. 2196–2204, 2017.

[25] M. Perez, M. Block, D. Espalin, R. Winker, T. Hoppe, F. Medina, and R. Wicker, "Sterilization of fdm-manufactured parts," in *Proceedings of the 2012 Annual International Solid Freeform Fabrication Symposium, Austin, TX, Aug*, 2012, pp. 6–8.

[26] A. Jokar and Z. Mohebbi, "Comparing the efficacy of alcohol isopropyl and ethanol on the reduction of contamination of medical check-up devices in children ward and neonatal intensive care unit (nicu)," *Int. Res. J. Pharm. Pharmacol*, vol. 1, p. 75, 2011.

[27] J. Xiao, Y. Zhang, J. Wang, W. Yu, W. Wang, and X. Ma, "Monitoring of Cell Viability and Proliferation in Hydrogel-Encapsulated System by Resazurin Assay," *Applied Biochemistry and Biotechnology*, vol. 162, no. 7, pp. 1996–2007, 2010.

[28] R. Lattouf, R. Younes, D. Lutomski, N. Naaman, G. Godeau, K. Senni, and S. Changotade, "Picrosirius Red Staining: A Useful Tool to Appraise Collagen Networks in Normal and Pathological Tissues," *Journal of Histochemistry and Cytochemistry*, vol. 62, no. 10, pp. 751–758, 2014.